JOURNAL OF GEOPHYSICAL RESEARCH, VOL. 94, NO. C3, PAGES 3255–3259, MARCH 15, 1989

The Underwater Noise of Rain

A. PROSPERETTI

Department of Mechanical Engineering, Johns Hopkins University, Baltimore, Maryland

L. A. CRUM AND H. C. PUMPHREY

National Center for Physical Acoustics, University, Mississippi

Numerous data on the spectra of underwater noise due to natural as well as artificial rain show a prominent and characteristic peak at a frequency around 14 kHz. It is argued that this acoustic emission is due to bubbles entrained in the liquid by the impact of raindrops. The mechanics of the entrainment is such that only drops in a narrowly defined size range have a high probability of entraining bubbles. The narrowness of this size range may explain why the 14-kHz peak is so ubiquitous and well defined.

INTRODUCTION

A rather remarkable feature of the underwater noise produced by rain, first noticed by *Scrimger* [1985], consists of a sharp spectral peak around 14 kHz. This structure is very clearly seen in Figure 1, which shows results from *Nystuen* [1986] and from *Scrimger et al.* [1987]. While the shape of the spectrum exhibits a strong dependence on rainfall rate and drop size distribution at lower frequencies, up to about 7 kHz, the 14-kHz peak retains essentially its characteristic shape and position, with increases or decreases of the rainfall rate merely affecting its magnitude. A modification of this structure occurs only in response to wind speed. While the peak rises very abruptly on the low-frequency side and has a rather narrowly defined maximum at low wind speeds (<1.2 m/s [*Scrimger et al.*, 1987]), these features become less sharply defined at higher wind speeds. More recent work by *Scrimger et al.* [1989] demonstrates that the 14-kHz peak is also observed for rainfall on the ocean and shows a gradual reduction in amplitude with increasing sea state.

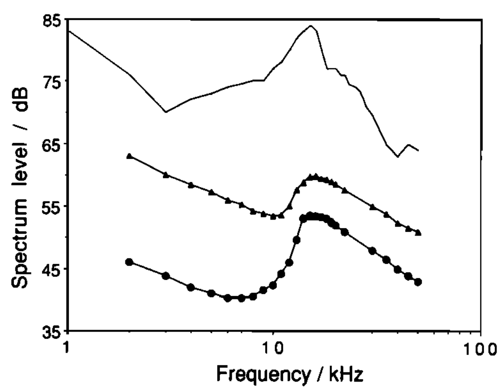

Fig. 1. Acoustic power spectra of rain falling on lakes, for very heavy rain (solid line [*Nystuen*, 1986]), light rain (triangles), and very light rain (solid circles [*Scrimger et al.*, 1987]). The spectrum level is in decibels referenced to 1μ Pa²/Hz.

We discovered that the peak could be surprisingly duplicated in the laboratory with artificial rainfall (Figure 2), even with a drop size distribution only moderately representative of natural rain. The artificial rain was made by producing a spray of drops from a tube containing several small holes. The smallest drops had a diameter of about 0.75 mm, and the largest ones had a diameter of about 1.5 mm; the maximum height of fall was about 1.5 m.

In the present paper we wish to suggest a mechanism for these unexpected findings. A consequence of the mechanism that we suggest is that this spectral peak is not very strongly correlated with the rainfall rate by itself. For the peak's level to become a useful indication of rainfall rate, the size distribution of the rain drops must also be known.

There are two mechanisms associated with drop impact upon a liquid surface that can produce sound. The first one is the impact itself. Although Nystuen attributes the 14-kHz peak to this process, we have rejected this mechanism for a variety of reasons [*Pumphrey and Crum*, 1988; *Pumphrey et al.*, 1989], some of which will become clear in the following discussions. The second process capable of generating sound is the entrainment in the liquid, under certain conditions, of an air bubble. At the moment of its formation this bubble is not in equilibrium but has some initial energy which is disposed of in the course of a series of damped free oscillations. While most of this initial energy is dissipated by thermal processes, a fraction is radiated as sound. In a classic and often-cited paper, *Franz* [1959] examined this bubble entrainment mechanism and found that when a bubble was formed, the resulting noise level was far greater than that due to the impact itself. However, since not every impact seemed to entrain a bubble,

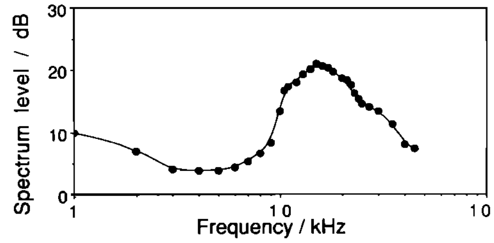

Fig. 2. Acoustic power spectrum of artificial rain falling onto a tank of water. The spectrum level is in decibels with an arbitrary reference level.

Paper number 88JC04284.
0148-0227/89/88JC04284$05.00

and since this process appeared to be random and irregular, he concluded that probably the major part of rain noise was due to the impact. We have repeated Franz's study reexamining in greater detail the entrainment process and have discovered an interesting effect that appears to explain the seemingly universal character of the 14-kHz peak associated with rainfall.

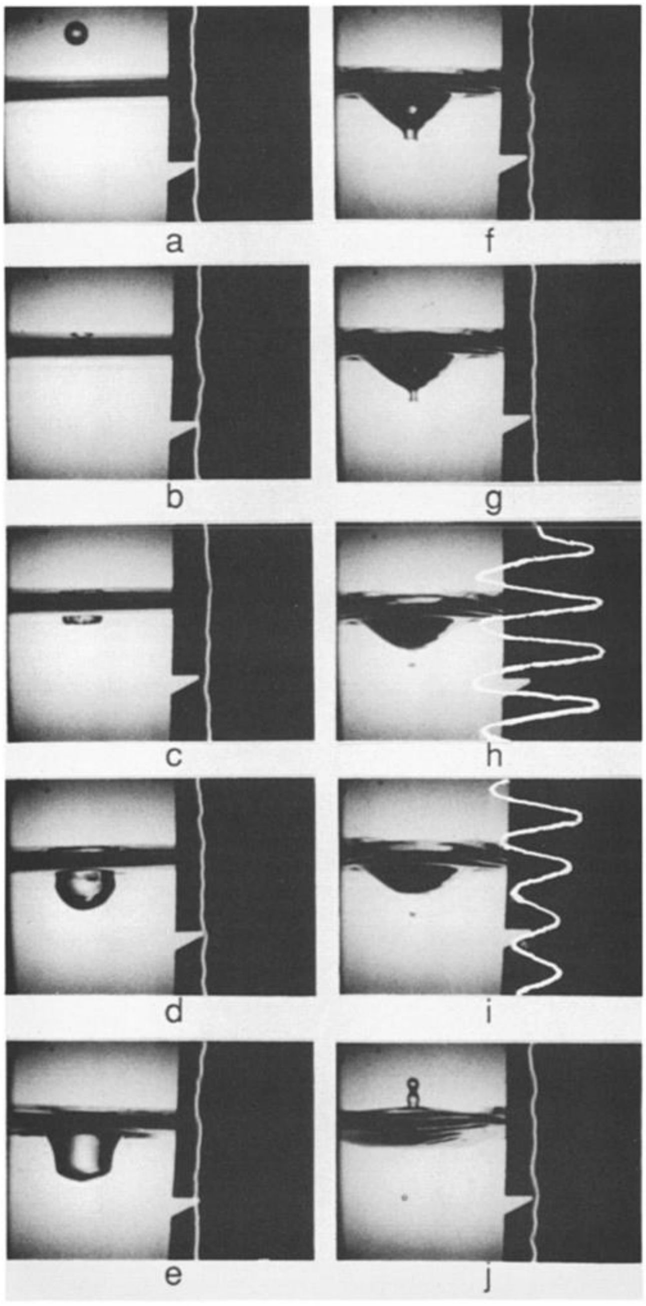

Fig. 3. Selected frames from a high-speed movie film, showing regular entrainment of bubbles. The original film was made at a speed of 2000 frames per second. The water drop (seen in Figure 3*a*) had a diameter of about 3 mm and an impact velocity of 2 m/s. The line down the right hand side of the film is an oscilloscope trace showing the acoustic pressure amplitude; in Figures 3*h* and 3*i* it was too faint to reproduce well and was touched up by hand. The damped sine wave in Figures 3*h* and 3*i* has a frequency of about 9 kHz, a frequency lower than that produced by raindrops at terminal velocity. Times after impact for each frame are as follows: (*a*): -3 ms, (*b*): 0 ms, (*c*): 2 ms, (*d*): 6.5 ms, (*e*): 14.5 ms, (*f*): 20 ms, (*g*): 20.5 ms, (*h*): 21 ms, (*i*): 21.5 ms, (*j*): 35.5 ms.

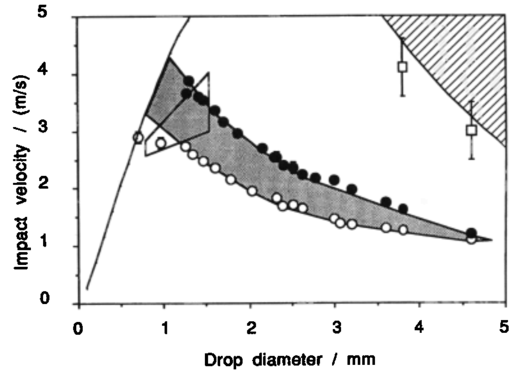

Fig. 4. Diagram showing the velocities and drop diameters for which bubbles are entrained. The stippled region in the center shows where regular entrainment occurs; its boundaries are simply curves drawn through the experimental points shown. Random or irregular entrainment tends to occur in the striped region in the upper right-hand corner of the figure. All but two of the data points used to draw the boundary of this region are off the edge of the figure. The curve at the left-hand side of the figure is the terminal velocity curve for raindrops while the four-sided figure below it outlines the region of the plot in which the artificial rain occurred.

BUBBLE FORMATION

We show in Figure 3 a series of high-speed photographs of a drop impact event which gives rise to the entrainment of a gas bubble. The time intervals between the pictures (which are sequential but not necessarily consecutive) are given in the caption. The vertical line on the right side of each frame is a picture of the "soundtrack" of the process obtained by simultaneously photographing the oscilloscope trace generated by a hydrophone placed in the vicinity of the impact point. It is evident that very little sound is associated with the impact itself (Figure 3*b*), while a very prominent signal appears as soon as the bubble detaches from the bottom of the crater produced by the impacting drop (Figure 3*h*). This observation conforms with the findings of Franz. What our results show, however, is that there is a range of drop sizes and impact velocities that gives rise to an entrained bubble for every impact. Outside this range, bubbles are never, or only irregularly, entrained.

The stippled area in Figure 4 represents the range of this regular entrainment process. The lines have been drawn by interpolating between the data points which are also shown. In the range below the stippled region the impact is not energetic enough to entrain a bubble, while above it the energy is excessive. At still higher velocities and diameters (upper right-hand corner), bubbles are entrained again, but now the process is random and irregular. This is the parameter range explored by Franz. Details of the experimental procedure by which these data were obtained are presented elsewhere [*Pumphrey and Crum*, 1988; *Pumphrey et al.*, 1989]. Briefly, drops with a diameter down to about 2 mm can be generated by means of a hypodermic needle. For a given drop size, the height of release was varied systematically to determine the threshold points shown in the figure. Smaller drops, down to about 1 mm in diameter, were obtained by lightly tapping a microliter syringe positioned at a fixed height above the liquid. In this case the threshold points were determined by systematically varying the amount of liquid released from the syringe. In both cases it was found that the thresholds were well defined and could be determined with little ambiguity.

According to the results of a number of photographic sequences similar to those shown in Figure 3 and to numerical simulations of the drop impact process (H. Oguz & A. Prosperetti, manuscript in preparation, 1989), the mechanism leading to bubble entrainment may be described as follows. When it hits, the drop imparts momentum to the liquid surface in all directions. At high impact velocities, this momentum is essentially equally distributed in all directions and the cavity grows more or less hemispherically. At lower impact velocities, however, the momentum imparted in the vertical direction is somewhat greater than that imparted in other directions. As a consequence, the outward liquid motion at the various points of the crater 's surface is arrested at different times in different directions. In particular, inversion of the liquid motion occurs latest at the bottom of the crater. This circumstance gives rise to the characteristic "nipple" that is clearly seen in Figure 3*f*. If the impact velocity is too low, this nipple does not last long enough to pinch off and form a bubble. As the impact velocity increases, however, the downward momentum increases, and pinching takes place. This situation corresponds to the lower boundary of Figure 4. As the impact velocity is increased further, the crater becomes wider and more nearly hemispherical, and inversion of the liquid outward flow starts taking place more and more simultaneously. As a consequence, the nipple cannot form, and no bubble is entrained. This corresponds to the upper boundary of the shaded region in Figure 4. At still higher impact velocities there is a possibility of bubble entrainment due not to the primary drop but to the secondary drop or drops produced by the capillary breakup of the jet that forms as a consequence of the filling of the crater. From a number of high-speed movies that we have analyzed, it seems that this event requires a rather precise timing of jet breakup and secondary drop impact. The need for such a precise synchronization of these elements has the effect that the entrainment of a bubble by this mechanism appears as a random, rather than deterministic, event.

A brief qualitative description of the characteristics of the entrained bubbles at the different points of the shaded region of Figure 4 is also useful for the following discussion. For impacts which are well inside the regular entrainment region, smaller drops give rise to smaller bubbles, although the decrease is less than proportional. For example, with a drop diameter of 4.3 mm and an impact velocity of 1.2 m/s, the entrained bubble has a radius of about 0.5 mm while a drop diameter of 2.25 mm and an impact velocity of 2.2 m/s produce a bubble of around 0.38 mm. For a fixed drop size, as the impact velocity is increased so as to traverse the shaded region in the vertical direction, the bubble starts at a relatively small size, rapidly gets bigger, and decreases in size again near the upper boundary. The bubble in Figure 3 is a good example; it was entrained by a 3-mm drop which impacted near the upper boundary. The bubble radius was about 0.35 mm, less than either of the above two examples. This variation of the entrained bubble radius with impact velocity can be as large as a factor of 2, but is very rapid near the boundaries of the shaded region. Therefore the great majority of the bubbles produced by drops of a given diameter impacting at different velocities has more or less the same size.

THE 14-KHZ PEAK

With the above considerations, we are now in a position to offer an explanation for the 14-kHz rain noise peak. The curve at the left of Figure 4 shows the terminal velocity of drops as a function of diameter. This line is a polynomial fit [*Dingle and Lee*, 1972] to some experimental data [*Gunn and Kinzer*, 1949]. It can be seen that the range of drop diameters where this terminal velocity curve intersects the shaded region corresponding to bubble entrainment is rather narrowly confined to 0.8 mm < *d* < 1.1 mm where *d* is the drop diameter. On the basis of the considerations given at the end of the preceding section, one can infer that the vast majority of the bubbles entrained by the impacts of these drops have a similarly narrowly defined size. A bubble of equilibrium radius R has a natural frequency f_o given to a rough approximation by Minnaert's formula [*Minnaert*, 1933; *Plesset and Prosperetti*, 1977]

$$f_o = \frac{1}{2\pi R}\left(\frac{3\gamma P_o}{\rho}\right)^{\frac{1}{2}}$$

where P_o is the ambient pressure, ρ is the liquid density, R is the bubble radius, and γ is the ratio of specific heats. For example, this formula gives f_o = 14.9 kHz for a radius R = 0.22 mm. A more precise calculation [*Prosperetti*, 1984; *Prosperetti et al.*, 1988] results in the very similar value f_o = 14.5 kHz for this value of R.

Although we have not been able to measure directly the size of the entrained bubbles in our artificial rain experiments, we found that the peak shown in Figure 2 resulted from the superposition of damped sinusoids having frequencies of around 14 kHz. The damping rate was consistent with the hypothesis that these signals were produced by bubbles in volume oscillation (H. C. Pumphrey and L. A. Crum, Free oscillations of near-surface bubbles as a source of underwater ambient noise, submitted to Journal of the Acoustical Society of America, 1989). Damped sinusoids having a higher frequency were also occasionally seen. It appears likely that these signals, which give rise to the high-frequency rolloff of the 14-kHz peak, are due to the smaller bubbles entrained by the droplets near the boundaries of the entrainment region as discussed at the end of the preceding section.

These considerations suggest that the 14-kHz peak is due to a rather narrowly defined droplet size range. When at terminal velocity, only drops in this range will entrain bubbles, and since bubble noise is so much more effective than the other noise production mechanisms, these drops lead to the formation of the peak. Drops in this size range happen to be present in almost any population of drops occurring in natural rain (see, for example, Figures 9 and 11 of *Scrimger et al.* [1987]), whence the seeming universality of the 14-kHz peak. The outlined area in Figure 4 shows the range of drop sizes and impact velocities for our artificial rain. It can be seen that drops close to the right size and velocity to cause the 14-kHz peak were also present here.

The experiments summarized in Figure 4 were conducted with the drops impacting normally on the liquid surface. It may be expected that plots similar to the one shown in this figure would be generated for any other angle of impact, with the bubble entrainment region depending on this angle. This may explain why the 14-kHz peak is found to be less sharp and more rounded in the presence of wind [*Scrimger et al.*, 1987] and gradually disappears as the sea state increases [*Scrimger et al.*, 1989]. Indeed, wind will both deflect the drop trajectories and produce water waves. Both elements will have an effect on the impact angle. As a consequence, a wider range of bubble sizes are generated and the sharp features of the peak are smeared.

The dynamics of crater growth and bubble entrainment are strongly dependent on surface tension. We have repeated our artificial rain experiments by adding to the water a small concentration of a surface-active agent. The spectra of Figure 5 and the photographs of Figure 6 show that the reduction of surface tension terminates bubble production and extinguishes sound radiation. A similar behavior has been found for natural rain [*Pumphrey, et al.*, 1989]. The exact mechanism leading to this effect is the object of current investigation.

CONCLUSIONS

The 14-kHz peak in the underwater sound intensity due to rainfall appears to be explained by the fact that a narrow range of raindrop sizes always entrains air bubbles upon impacting a water surface at their terminal velocity. This restricted range of drop sizes also restricts the size of the bubbles entrained and therefore (through the well-known relation between bubble size and frequency of oscillation) leads to a peak in the spectral intensity, the position of which is essentially independent of other conditions. If this explanation is correct, it is clear that observation of the 14-kHz peak essentially monitors a narrow segment of the drop size distribution and therefore by itself cannot be correlated with the total rainfall rate. For this purpose, the size distribution of the raindrops must also be known. Another interesting conclusion may be drawn from the fact that the 14-kHz peak is typically 15–20 dB above the noise level at lower frequencies. This circumstance seems to indicate that even though only a small fraction of drops are capable of entraining bubbles, their acoustic effect is nevertheless dominant. It may therefore be concluded that ambient noise in the ocean, even in other frequency regions, may be very strongly influenced by those processes capable of entraining bubbles. Breaking waves, both in the spilling and plunging mode, are obvious examples.

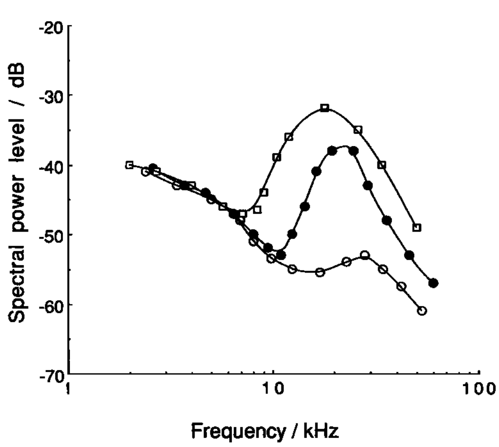

Fig. 5. Variation of the power spectrum of artificial rain with surfactant concentration. Open squares indicate clean water with surface tension of 72 mN / m (= 72 dyn / cm). Solid circles indicate surface tension of 61 mN / m. Open circles indicate surface tension of 41 mN / m. The decibel reference level is arbitrary.

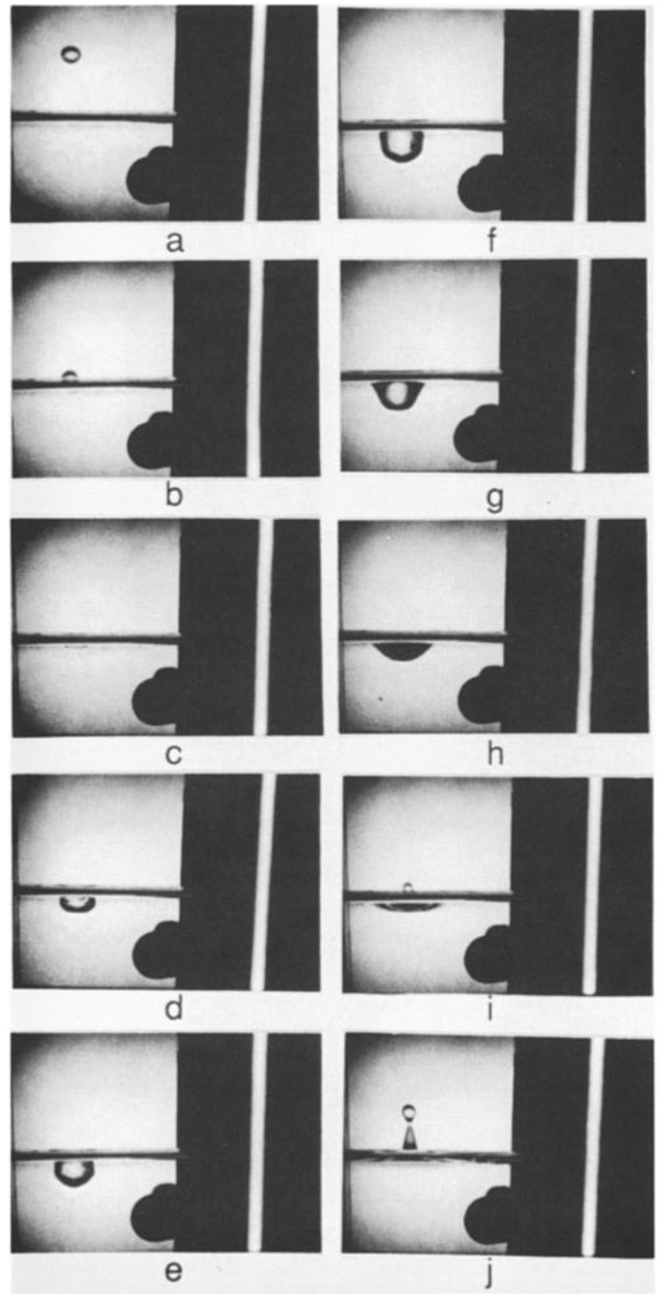

Fig. 6. Selected frames from a high-speed movie showing a drop of 3.8-mm diameter impacting at 1.5 m/s. With clean water these parameters lead to regular entrainment, as in Figure 3, but in this case a surfactant has been added to the water. This prevents a bubble from being entrained, and consequently no sound is produced. The original movie was taken at a speed of 1000 frames per second. Times after impact for each frame are as follows: (*a*): -9 ms, (*b*): -1 ms, (*c*): 1 ms, (*d*): 5 ms, (*e*): 8 ms, (*f*): 13 ms, (*g*): 20 ms, (*h*): 27 ms, (*i*): 35 ms, (*j*): 57 ms.

Acknowledgment. This study has been supported by the Ocean Acoustics Branch of the Office of Naval Research.

REFERENCES

Dingle, A. N., and Y. Lee, Terminal fallspeeds of raindrops, *J. Appl. Meteorol.*, *11*, 877–879, 1972.

Franz, G. J., Splashes as sources of sound in liquids, *J. Acoust. Soc. Am.*, 31, 1080–1096, 1959.

Gunn, R., and G. D. Kinzer, The terminal velocity of fall for water droplets in stagnant air, *J. Meteorol.*, *6*, 243–248, 1949.

Minnaert, M., On musical air-bubbles and the sounds of running water, *Philos. Mag.*, *16*, 235–248, 1933.

Nystuen, J. A., Rainfall measurements using underwater ambient noise, *J. Acoust. Soc. Am.*, *79*, 972–982, 1986.

Plesset, M. S., and A. Prosperetti, Bubble dynamics and cavitation, *Annu. Rev. Fluid. Mech.*, *9*, 145–185, 1977.

Prosperetti, A., Bubble phenomena in sound fields, *Ultrasonics*, *22*, 69–77, 1984.

Prosperetti, A., L. A. Crum, and K. Commander, Nonlinear bubble dynamics, *J. Acoust. Soc. Am.*, *83*, 502–514, 1988.

Pumphrey, H. C. and L. A. Crum, Acoustic emissions associated with drop impacts, in *Sea Surface Sound*, edited by B.R. Kerman, pp.463–483, Kluwer, Norwell, Mass., 1988.

Pumphrey, H. C., L. A. Crum and L. Bjørnø, Underwater sound produced by individual drop impacts and rainfall, *J. Acoust. Soc. Am.*, in press, 1989.

Scrimger, J. A., Underwater noise caused by precipitation, *Nature*, *318*, 647–649, 1985.

Scrimger, J. A., D. J. Evans, G. A. McBean, D. M. Farmer and B. R. Kerman, Underwater noise due to rain, hail and snow, *J. Acoust. Soc. Am.* *81*, 79–86, 1987.

Scrimger, J. A., D. J. Evans, and W. Yee, Underwater noise due to rain–Open ocean measurements. *J. Acoust. Soc. Am.*, in press, 1989.

L. A. Crum and H. C. Pumphrey, National Center for Physical Acoustics, P.O. Box 847, University, MS 38677.

A. Prosperetti, Department of Mechanical Engineering, Johns Hopkins University, Baltimore, MD 21218.

(Received July 26, 1988;
accepted September 28, 1988.)